Vacancy defects in epitaxial thin film $CuGaSe_2$ and $CuInSe_2$

E. Korhonen, K. Kuitunen, and F. Tuomisto
Department of Applied Physics, Aalto University, P.O. Box 11100, Aalto FI-00076, Finland

A. Urbaniak and M. Igalson
Faculty of Physics, Warsaw University of Technology, Koszykowa 75, Warszawa PL 00 662, Poland

J. Larsen, L. Gütay, and S. Siebentritt
University of Luxembourg, Belvaux L-4422, Luxembourg

Y. Tomm
Helmholtz Centre Berlin for Materials and Energy, Berlin D-14109, Germany
(Received 18 August 2011; revised manuscript received 30 May 2012; published 6 August 2012)

Epitaxial thin film $CuGaSe_2$ and $CuInSe_2$ samples grown on GaAs substrates with varying [Cu]/[Ga,In] ratios were studied using positron annihilation Doppler-broadening spectroscopy and were compared to bulk crystals. We find both Cu monovacancies and Cu-Se divacancies in $CuInSe_2$, whereas, in $CuGaSe_2$, the only observed vacancy defect is the Cu-Se divacancy.

DOI: 10.1103/PhysRevB.86.064102 PACS number(s): 88.40.jn, 61.72.jd, 78.70.Bj

I. INTRODUCTION

Ternary compounds Cu(In,Ga)Se_2 (CIGS) are used as absorbers in thin film photovoltaics. CIGS-based solar cells represent the most efficient technology for thin film photovoltaics available today, achieving efficiencies above 20% with laboratory cells.[1] Although the technology is practically usable, knowledge of several basic properties relating to defects and doping of the material is still limited.[2]

The doping in chalcopyrites is believed to be caused by native defects, such as vacancies and antisites. These can have both donor and acceptor characters, and they can compensate each other, although the sum effect is usually a *p*-type CIGS absorber. The doping affects the band bending, the built-in voltage, and finally, the open circuit voltage and the efficiency of photovoltaic conversion. Defects also act as recombination centers, which are detrimental to the efficiency.

Chalcopyrite-based solar cells show metastabilities created by light soaking or voltage pulsing.[3,4] These are known to affect the net acceptor concentration and capacitance of the junction and as such, the efficiency of the photovoltaic conversion. Generally, light soaking is considered to be a positive effect, which relaxes away in the dark during a time span of several hours. This does cause the efficiency to be dependent on the history of the cell, which is an important problem in practical use.[2] The metastable behavior has been attributed based on theoretical calculations at least partially to the V_{Se} and V_{Cu}-V_{Se} vacancies.[3,5]

In this paper, we use positron annihilation spectroscopy to study CGS and CIS thin films with varying Cu/Ga and Cu/In compositions, respectively. The goal is to gain further insight into the identities and concentrations of vacancy defects present in CIGS materials depending on growth conditions. Preliminary results have been reported in CIS by Niki *et al.*[6] and in CGS by Islam *et al.*,[7] but conclusive evidence about the nature of the vacancy defects in high-quality epitaxial CGS/CIS thin films is lacking.

II. SAMPLE PREPARATION AND EXPERIMENTAL TECHNIQUES

A. Sample preparation and photoluminescence

The epitaxial CIS and CGS samples were grown by metal organic vapor phase epitaxy (MOVPE) on "epiready" semi-insulating and Zn-doped GaAs (001) wafers in an Aixtron AIX200 MOVPE reactor at 50-mbar pressure. As precursors, we used cyclopentadienyl- copper-triethyl-phosphine, triethyl-gallium, trimethyl-indium, and ditertiary-butyl-selenide. The thickness of the deposited films is either 400 or 800 nm, depending on the process. The growth temperature is 570 °C for CGS layers and 470 °C for the CIS layers. Films grow with the *c* axis perpendicular to the surface. A detailed description of the growth process and the resulting structure of the grown samples can be found in Ref. 8. All samples have been etched for 2 min in 5% potassium cyanide to remove the secondary Cu_xSe phase that appears at the surface under Cu-rich growth conditions. Compositions of the samples were determined using photoluminescence (PL) (see Sec. III) and are presented in Table I. The compositions were also checked by energy-dispersive x-ray spectroscopy (EDX), however, EDX is not very reliable for these thin films, and PL fingerprints, as discussed in Sec. III, proved to be much more reliable and comparable.

For both $CuInSe_2$ and $CuGaSe_2$, a clear relation between the PL spectrum and the composition exists:[9,10] In material grown under Cu excess, two donor-acceptor transitions are observed, the relative intensity of which depends on the Cu excess. Cu-poor material shows an asymmetrically broadened emission, which shifts red for the increasing Cu deficit.

The bulk crystals were grown by the Bridgman method and were measured by EDX and by PL to be Cu rich. Thin slabs were cut from the ingots and were etched in potassium cyanide to remove the Cu_xSe secondary phase.

PL measurements were performed using the 514.5-nm line of an Ar^+ laser to excite samples cooled to 10 K in a helium

 ©2012 American Physical Society

TABLE I. Sample information.

CGS	[Cu/Ga]	CIS	[Cu/In]
No. 1	1.2	No. 1	1.2
No. 2	1.2	No. 2	1.2
No. 3	1.2	No. 3	1.2
No. 4	1.15	No. 4	1.15
No. 5	1.1	No. 5	1.1
No. 6	1.1	No. 6	1.0
No. 7	1.0	No. 7	0.9
No. 8	0.8	No. 8	0.8
No. 9	0.6		

cryostat. Photon excitation fluxes of 10^{19} s^{-1} cm^{-2} were used in PL studies. The emitted luminescence was detected with an Andor Shamrock 303 spectrograph equipped with a Si and an InGaAs detector array. The system is corrected for the spectral efficiency of all optical elements, including filters, lenses, grids, and detectors.

B. Positron experiments

The chalcopyrite CIGS samples were studied using positron annihilation spectroscopy, a versatile tool for studying vacancy-type defects.[11] By using a monoenergetic slow positron beam, the implantation energy and, hence, the depth distribution can be controlled for thin film experiments. Implantation energies used ranged from 1 to 35 keV, which probe the samples from a few nanometers below the surface to approximately 3 μm. This allows defect distribution profiling. Implanted positrons thermalize within a few picoseconds and afterwards diffuse in the sample until annihilating with an electron. Positrons are repelled by atom cores, which leads to neutral and positive vacancy-type defects acting as positron traps. Typical lifetimes are in the range of 100–250 ps, and the diffusion length varies from a few nanometers to hundreds of nanometers, both heavily dependent on the type and concentration of vacancies.

In Doppler-broadening spectroscopy, one measures the Doppler broadening of the 511-keV positron-electron annihilation radiation peak. This broadening is caused mainly by the momentum of the annihilating electrons. Two Ge detectors with an energy resolution of 1.3 keV at 511 keV were used for measuring the spectrum. To describe the spectrum in a brief fashion, two parameters S and W are typically used. The low-momentum parameter S is the fraction of counts in the central region of the peak, whereas, W corresponds to the fraction of counts in the wing areas on both sides of the peak. The W parameter is more sensitive to highly localized core electrons. The integration windows are set symmetrically around the peak. In this paper, annihilations corresponding to longitudinal momentum [−0.44–0.44 a.u.] ([−3.2–3.2] $\times 10^{-3} m_0 c$) define the S parameter. The W windows were set as ±[1.6–4.0] a.u. (±[11.4–28.9] $\times 10^{-3} m_0 c$). Typically, an increase in the value of S indicates an increase in open volume defects in the depth being probed. The value of W is more dependent on the type of atoms surrounding the annihilation site.

The measured values for S and W result from annihilations in different states and as such, are superpositions from the individual values. In the case of only two positron annihilation states, the resulting S and W can be expressed as

$$S = \eta_1 S_1 + \eta_2 S_2, \tag{1}$$

$$W = \eta_1 W_1 + \eta_2 W_2, \tag{2}$$

where η_1 and η_2 are annihilation fractions in the relevant states ($\eta_1 + \eta_2 = 1$). In the S-W plane, the above equations would draw a line segment between (S_1, W_1) and (S_2, W_2) if only the fractions were to change. In the case of more than one type of defect, the behavior would be nonlinear.

If the lattice is dominated by only one type of vacancy defect (D) in addition to the free positron state (B), a new parameter can be defined[11]

$$R = \left|\frac{\Delta S}{\Delta W}\right| = \left|\frac{S - S_B}{W - W_B}\right| = \left|\frac{S_D - S_B}{W_D - W_B}\right|, \tag{3}$$

which is independent of the annihilation fraction and, thus, characterizes the defect in relation to the bulk. It essentially describes the slope of the characteristic line in the (S, W) plot. In this case, the trapping rate to defect κ_D can be calculated with

$$\kappa_D = \mu_D c_D = \lambda_B \frac{W - W_D}{W_D - W} = \lambda_B \frac{S - S_B}{S_D - S}, \tag{4}$$

where λ_B is the decay constant of the bulk state. μ_D and c_D are the trapping coefficient and the concentration of vacancies, respectively. Using Eq. (4) with measured Doppler parameters and bulk lifetime and using the trapping rate coefficient typical of cation-type defects in compound semiconductors[11] ($\mu_D = 3 \times 10^{15}$ s^{-1}), the vacancy concentration can be estimated in the range of 10^{15}–10^{19} cm^{-3}.

III. PHOTOLUMINESCENCE CHARACTERIZATION

PL is applied in this paper to determine the composition of the samples. This is achieved by interpretation of the measured PL spectra in terms of the defect model for CGS presented in the paper by Bauknecht *et al.*[12]

Figure 1 shows examples of PL spectra from samples used in this paper with different stoichiometries. According to Ref. 12, two donor-acceptor (DA) transitions can be observed in stoichiometric and Cu-rich CGS. These are observed in samples grown under Cu-rich conditions investigated in this paper. A DA transition, named DA2, with a peak energy of 1.62 eV dominates in Cu-rich material ([Cu]/[Ga] $\geqslant$ 1.2. This is the case for sample No. 2 in Fig. 1, which can, therefore, be classified as [Cu]/[Ga] $\geqslant$ 1.2. Another DA, with a transition energy of 1.66 eV, called DA1, dominates in near-stoichiometric slightly Cu-rich material [Cu]/[Ga] $\approx$ 1. This transition dominates in sample No. 7. For material with [Cu]/[Ga] between 1 and 1.2, such as sample No. 6, the composition of the samples is estimated from the ratio of the DA1 and DA2 peaks. Applying this procedure, we determine that sample No. 6 has a higher [Cu]/[Ga] ratio than sample No. 7. A third DA, labeled DA3 in Fig. 1 is observed in several samples. This has, however, not been related to the composition and is, therefore, not analyzed here.[9]

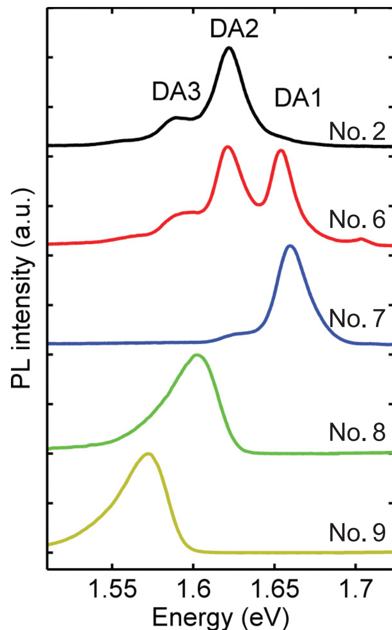

FIG. 1. (Color online) PL spectrum of selected samples with different compositions.

The PL signal recorded from Cu-poor CGS shows a very typical behavior for highly compensated semiconductors with fluctuating potentials. The peak is asymmetrically broadened and is shifted to lower energies than the DA1.[12] A lower energetic peak position and broader peaks are signs of increased compensation. This is a direct measure of composition since the decrease in Cu content increases the compensation. Samples Nos. 8 and 9 in Fig. 1 are examples of typical PL spectra for the Cu-poor samples. Based on the lower energetic position of sample No. 9 relative to No. 8, it is determined that No. 9 has the highest Cu deficiency. The assignment of the peaks was, in all cases, verified by intensity-dependent PL studies where all peaks show behavior that is in accordance with the model described in Ref. 12. The spectra of all samples were not shown in Fig. 1, but the relative compositions of all samples were determined in accordance with this model.

The approach to determine the relative composition of the CIS samples is the same. The interpretation of the results is based on the defect model presented by Siebentritt *et al.*[10] The defects and their compositional dependence observed in CIS are the same as observed in CGS, only the energies of the transitions in CIS are lower due to the lower band gap. In CIS, the DA1 is observed at 0.99 eV, and the DA2 is observed at 0.97 eV. The relative composition of the CIS samples is, therefore, determined as explained for CGS. The absolute composition values given in Table I are estimated by comparison to energy-dispersive x-ray spectroscopy measurements.

It has to be noted that Cu-rich CIGS is not a single phase material, it consists of stoichiometric CIGS plus Cu selenides. The Cu selenide secondary phase is etched, so the material we look at is stoichiometric, i.e., [Cu]/[III] = 1. However, as is obvious from the PL spectra, the defect structure depends on the Cu excess during growth. The [Cu]/[III] ratio given is the average overall composition before etching.

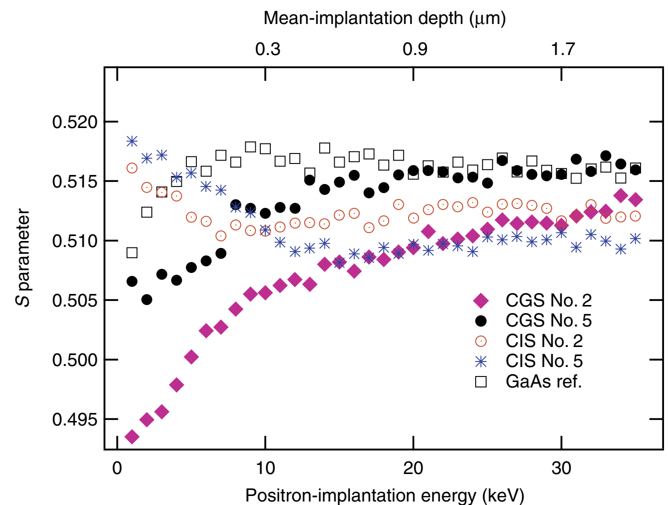

FIG. 2. (Color online) Low-momentum parameter S as a function of implantation energy in selected CGS and CIS samples. Mean-implantation depth is also shown.

IV. VACANCY IDENTIFICATION

A. Results

Figure 2 shows the low-momentum parameter S as a function of implantation energy plotted for a selection of CGS and CIS samples as well as the p-type GaAs reference sample. The corresponding mean-implantation depth is marked on the top axis. The curves exhibit a similar form: S starts at a surface value and then slowly approaches the bulk crystal value. At low energies ($E < 3$ keV), the effect of surface annihilations dominates and gives a distinct (S,W) value. For most of the CGS samples, the surface value of S is lower than the bulk value. For all of the CIS samples, the S starts high compared to the bulk value. This difference is caused by the different densities and types of surface states and oxides on these two materials. It should be noted that the width of the implantation distribution is roughly the same as the mean depth, so the annihilation parameters should change smoothly when the implantation energy is increased to values high enough to reach the GaAs substrate. In this paper, we are interested in the annihilation parameters of the $C(I,G)Se_2$ layers, which are 400–800-nm thick. Because of the surface effects and the transition into the GaAs substrate, representative values for the layer S and W parameters are found in the implantation energy region of 5–15 keV. To better visualize the change in Doppler parameters in the different samples, the annihilation parameter values in the film depth were plotted in the S-W plane. Data points were selected for each sample from an energy range where S and/or W were roughly constant, best describing the layer.

The data obtained in the CGS layers are illustrated in Fig. 3. In addition, the data point measured in a CGS bulk crystal is shown. A line with a slope of -0.5 can be fitted through the data points, which corresponds to $R = 2.0$. This indicates that positrons annihilate in two different states in the samples. A general trend of increasing S and decreasing W with the decreasing [Cu]/[Ga] ratio can be observed, indicating an increasing vacancy concentration with a decreasing [Cu]/[Ga] ratio. For comparison, the data point for the defect-free ZnSe

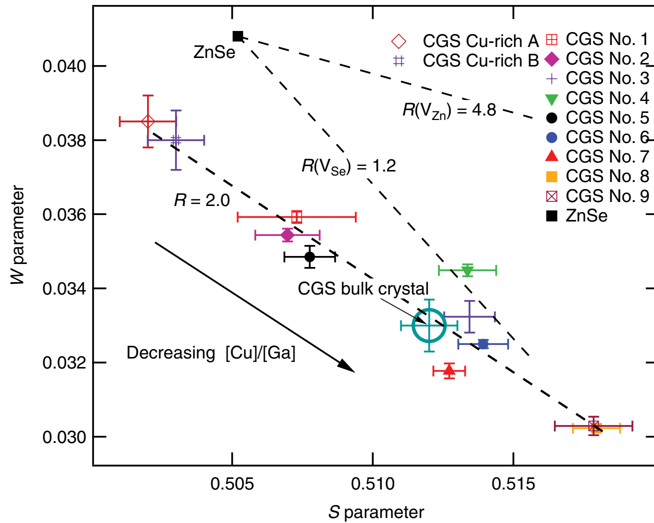

FIG. 3. (Color online) S-W plot of $CuGaSe_2$ samples. Each sample is represented by one point. Samples A and B were grown in similar Cu-rich conditions as Nos. 1 to 3, but the actual [Cu]/[Ga] ratio has not been determined by PL.

reference is presented together with the slopes corresponding to cation (V_{Zn}) and anion (V_{Se}) vacancies.[13] The comparison is relevant as the atomic structure of ZnSe is very similar to CGS, and the Cu and Ga core-electron distributions are very similar to Zn (positrons are very sensitive to the $3d$ electrons in these systems). The R values for these vacancies are $R(V_{Zn}) = 4.8$ and $R(V_{Se}) = 1.2$, respectively. The comparison suggests that the defects observed in the CGS samples have the nature of both cation and anion vacancies.

Figure 4 shows the S,W data for the CIS layers and a p-type CIS bulk crystal. The data points seem to form two distinct lines with slopes of -0.2 (corresponding to $R_1 = 4.6$) and -0.6 ($R_2 = 1.8$). The different behavior compared to CGS indicates that positrons annihilate from at least three different states (at least two kinds of vacancy defects) in these samples. Also here, a general trend of increasing S

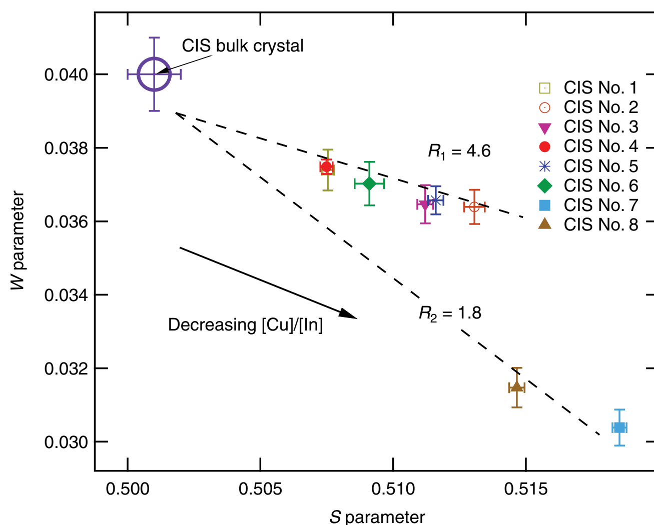

FIG. 4. (Color online) S-W plot of $CuInSe_2$ samples. Each sample is represented by one point.

and decreasing W with a decreasing [Cu]/[In] ratio can be observed, indicating an increasing vacancy concentration with a decreasing [Cu]/[In] ratio, although the correlation is less clear than in CGS.

B. Discussion

1. $CuGaSe_2$

Comparing the CGS data in Fig. 3 to ZnSe shows that the R parameter of CGS is halfway between the anion and the cation vacancies in ZnSe, making the divacancy V_{Cu}-V_{Se} in CGS a natural suggestion for the dominant defect responsible for positron trapping. Furthermore, from the span of the S (0.502–0.520) and W (0.030–0.039) parameters measured in all the samples along the line, one can deduct that the defect-specific parameters of the observed vacancy defect are $S_v \geqslant 1.036 \times S_b$ and $W_v \leqslant 0.77 W_b$, where S_b and W_b are the values corresponding to the perfect lattice. Comparison to values for similar III-V and II-VI semiconductors where cations and anions are size matched, namely, GaAs and ZnSe, where native cation and anion vacancies have $S_v < 1.03 \times S_b$ and $W_v > 0.8 W_b$,[13,14] supports the conclusion that the observed defects are larger than monovacancies on any lattice site in CGS.

We also measured the positron lifetime in a melt-grown[15] $CuGaSe_2$ bulk crystal: The average positron lifetime in this sample is $\tau_{ave} = 280$ ps. A simple decomposition of the lifetime spectrum into two components was not possible, but the longest lifetime component in the spectrum is $\tau_D = 320 \pm 25$ ps with significant intensity. The difficulty in the decomposition is probably due to the presence of a nonvanishing concentration of smaller vacancy defects, which are not dominant trapping centers but affect the spectrum enough to make a proper decomposition impossible. The lifetime in the perfect lattice (called bulk lifetime) in ZnSe is $\tau_b = 240$ ps,[16] and since the lattice constants, structure, and the constituent atoms are very similar in ZnSe and $CuGaSe_2$, it can also be assumed that $\tau_b \approx 240$ ps in CGS. To get some insight into the vacancy-specific lifetimes, we calculated the positron lifetimes by solving the positron state and constructing the electron density of the wave function of the free atoms, similarly as described in Ref. 17. Similarly, as in Ref. 16 for ZnSe, the results of the calculations show that the positron lifetime of Cu and Ga vacancies is only $\tau_v - \tau_b = 10$–20 ps longer than in the lattice, whereas, for the Se vacancy in the relaxed state[3] and for the divacancy, the lifetime difference is $\tau_v - \tau_b = 60$–80 ps.

The above observations clearly suggest that the dominant vacancy defect that traps positrons in all the CGS samples is the divacancy V_{Cu}-V_{Se}. Furthermore, based on the position of the melt-grown CGS sample (in which the average lifetime indicates that the fraction of positron annihilating at the divacancies is roughly 50%) on the line in Fig. 3, it seems plausible that positrons are not trapped at vacancies (meaning that their concentration is less than 10^{18} cm^{-3}) in the CGS thin films with the highest (grown under Cu excess) [Cu]/[Ga] ratios. Applying the standard trapping model,[11] we can estimate the concentrations of the vacancies to be in the 10^{17}–10^{18} cm^{-3} range in the other samples. It should, however, be noted that positrons are only sensitive to those defects that are in the negative and neutral charge states.

2. $CuInSe_2$

Due to the different nature of 3d and 4d electrons in Ga and In, respectively, and their different effects on positron data,[11] the data from the CIS samples cannot be compared as straightforwardly to ZnSe as in the case of CGS. Two characteristic R parameters can be identified, $R_1 = 4.6$ and $R_2 = 1.8$. In both cases, the data points move towards the lower right corner, i.e., higher defect densities with decreasing [Cu]/[In], suggesting the involvement of V_{Cu} in both vacancy defects observed. The data point in the upper left corner is measured in a p-type $CuInSe_2$ bulk crystal that exhibits a single positron lifetime of $\tau_b = 240$ ps. By comparing to CGS and ZnSe, this lifetime can be interpreted as the bulk lifetime in $CuInSe_2$—hence, the S and W parameters measured in this sample represent the lattice, i.e., positron trapping at vacancies is not observed in this sample.

Analyzing the S and W parameter ranges in the two slopes gives $S_v \geqslant 1.036 \times S_b$ and $W_v \leqslant 0.75 W_b$ for $R_2 = 1.8$ and $S_v \geqslant 1.024 \times S_b$ and $W_v \leqslant 0.90 W_b$ for $R_1 = 4.6$. With similar arguments as in the case of CGS, the former requires vacancy defects larger than monovacancies (e.g., divacancies), whereas, a monovacancy-sized defect could explain the latter. Hence, we suggest that, in the CIS layers with the lowest [Cu]/[In] ratio, the dominant vacancy defects that trap positrons are V_{Cu}-V_{Se} divacancies, whereas, V_{Cu} monovacancy-type defects dominate at higher [Cu]/[In] ratios. The lower R for V_{Cu}-V_{Se} in CIS than CGS can be explained by the In 4d electrons giving a less important contribution in the high-momentum area of the annihilation peak, leading to a lower W parameter.

According to theoretical calculations for Se-poor and Cu-rich CGS and CIS,[3] the formation energy of V_{Cu} is less than that of V_{Se}, and the divacancy is energetically favorable. Furthermore, Cu migrates relatively easily in CIS,[18] so it seems plausible that an excess of Cu vacancies exists in the material which can diffuse in the sample and can find all of the Se vacancies to form energetically favorable V_{Cu}-V_{Se}. The remaining V_{Cu} can either disappear through the surfaces or be bound by some other defects. Eventually, it is the concentration and charge state balance between the two kinds of defects that dictate which is the dominant defect that traps positrons. In CGS and Cu-poor CIS, it seems to be the V_{Cu}-V_{Se} divacancy, whereas, the single V_{Cu} dominates in Cu-rich CIS. Applying the standard trapping model,[11] we can estimate the concentrations of these vacancies to be in the 10^{17}–10^{18}-cm^{-3} range in the thin films. It should, however, be noted again that positrons are only sensitive to those defects that are in the negative and neutral charge states.

V. SUMMARY

We present results obtained with positron annihilation spectroscopy in thin film CIGS solar cell materials. We show that monovacancies and divacancies are present in the materials in high concentrations. The concentrations of these vacancy defects are in the 10^{17}–10^{18}-cm^3 range. In $CuGaSe_2$, V_{Cu}-V_{Se} divacancies are observed with concentrations varying as a function of the [Cu]/[Ga] ratio, whereas, both V_{Cu}-V_{Se} divacancies and V_{Cu} are found in $CuInSe_2$, depending on the [Cu]/[In] ratio. In Cu-poor $CuInSe_2$, the divacancy dominates. Solar cells are made from Cu-poor absorbers. Thus, these measurements indicate a high concentration of Cu-Se divacancies in solar cell relevant material. Hence, divacancies can be responsible for the observed metastable effects.

ACKNOWLEDGMENTS

This work was performed as part of a MATERA ERA-NET project cofunded by the Fonds National de la Recherche Luxembourg (FNR), the Polish National Centre for Research and Development (NCBiR), and the Academy of Finland.

[1] P. Jackson, D. Hariskos, E. Lotter, S. Paetel, R. Wuerz, R. Menner, W. Wischmann, and M. Powalla, Prog. Photovoltaics **19**, 894 (2011).

[2] S. Siebentritt, M. Igalson, C. Persson, and S. Lany, Prog. Photovoltaics **18**, 390 (2009).

[3] S. Lany and A. Zunger, J. Appl. Phys. **100**, 113725 (2006).

[4] M. Igalson, in *Metastable Defect Distributions in CIGS Solar Cells and Their Impact on Device Efficiency*, MRS Symposia Proceedings No. 1012 (Cambridge University Press, Cambridge, UK, 2007), p. 211.

[5] S. Lany and A. Zunger, Phys. Rev. B **72**, 035215 (2005).

[6] S. Niki, R. Suzuki, S. Ishibashi, T. Ohdaira, P. J. Fons, A. Yamada, H. Oyanagi, T. Wada, R. Kimura, and T. Nakada, Thin Solid Films **387**, 129 (2001).

[7] M. M. Islam, A. Uedono, S. Ishibashi, K. Tenjinbayashi, T. Sakurai, A. Yamada, S. Ishizuka, K. Matsubara, S. Niki, and K. Akimto, Appl. Phys. Lett. **98**, 112105 (2011).

[8] L. Gütay, J. Larsen, J. Guillot, M. Müller, F. Bertram, J. Christen, and S. Siebentritt, J. Cryst. Growth **315**, 82 (2011).

[9] S. Siebentritt, I. Beckers, T. Riemann, J. Christen, A. Hoffmann, and M. Dworzak, Appl. Phys. Lett. **86**, 091909 (2009).

[10] S. Siebentritt, N. Rega, A. Zajogin, and M. C. Lux-Steiner, Phys. Status Solidi C **1**, 2304 (2004).

[11] K. Saarinen, P. Hautojärvi, and C. Corbel, in *Identification of Defects in Semiconductors*, edited by M. Stavola (Academic, San Diego, 1998), pp. 209–85.

[12] A. Bauknecht, S. Siebentritt, J. Albert, and M. C. Lux-Steiner, J. Appl. Phys. **89**, 4391 (2001).

[13] K. Saarinen, T. Laine, K. Skog, J. Mäkinen, P. Hautojärvi, K. Rakennus, P. Uusimaa, A. Salokatve, and M. Pessa, Phys. Rev. Lett. **77**, 3407 (1996).

[14] K. Saarinen, S. Kuisma, P. Hautojärvi, C. Corbel, and C. LeBerre, Phys. Rev. B **49**, 8005 (1994).

[15] T. F. Ciszek, J. Cryst. Growth **79**, 689 (1986).

[16] J. Gebauer, R. Krause-Rehberg, M. Prokesch, and K. Irmscher, Phys. Rev. B **66**, 115206 (2002).

[17] M. Hakala, M. J. Puska, and R. M. Nieminen, Phys. Rev. B **57**, 7621 (1998).

[18] K. Gartsman, L. Chernyak, V. Lyahovitskaya, D. Cahen, V. Didik, V. Kozlovsky, R. Malkovich, E. Skoryatina, and V. Usacheva, J. Appl. Phys. **82**, 4282 (1997).